RESEARCH ARTICLE OPEN ACCESS

Synthesis & Characterization of Fluorescent Silver Nanoparticles stabilized by *Tinospora Cordifolia* leaf Extract-A Green Procedure

M. Padma, [1] Boddeti Govindh,[2] B. Venkateswara Rao[1]*
[1]*Department of Engineering Chemistry, College of Engineering, Andhra University, Visakhapatnam, India-530003. Telephone: (O) 0891-2844916.
[2]Dairy Animal Husbandry Research Centre, Visakha Dairy Training Centre, Visakhapatnam-530040.

Abstract:
Synthesis of silver nanoparticles (Ag-NPs) was achieved by a simple green procedure using *Tinospora Cordifolia* leaf extract as stabilizer/reducing agents. Ag-NPs in the size range of 2–19 nm is obtained by the treatment of aqueous silver ions with leaf extracts of *Tinospora Cordifolia.* This eco-friendly approach is simple, amenable for large scale commercial production and technical applications. Further, photoluminiscence studies of these Ag-NPs were recorded & suggested that the present particles were suitable for fluorescence emitting probes. These red emitting Ag-NPs exhibited distinct fluorescence properties (both emission and stokeshift).

I. Introduction

Now-a-days, the potential of various microbes and plant biomasses for the synthesis of nanometals was explored. Sastry and co-workers examined the possibility of using microbes and plant materials as nano-factories [1–6]. Since then, various plant extracts and microorganisms have been employed for the synthesis of nanoparticles in eco-frindly manner instead of chemical and physical methods. In recent years, the biosynthetic method using plant extracts has received more attention than the use of microbes for the nano-scale metal synthesis because plant materials for the synthesis of nanoparticles does not perform elaborative processes such as the maintaince of cell cultures [7-13]. In very recent years, the use of these biosynthesized nanomaterials has received much attention in the fields of catalysis and optics.

On the other hand, the metal nanoparticles display novel physical and chemical properties due to surface effect, where most of the particle atoms are just surface atoms. Thus, these metal nanoparticles have attracted significant attention due to their interesting optical and electronics properties, which have resulted in the exploitation of a number of applications in chemistry and in biochemistry [14-19]. The size and shape of nanoparticles can modulate fluorescence of a target dye close to the metal surface. The enhancement of the fluorescence efficiency is due to dipole moment with surface plasmons [20–23]. The optical properties of metal nanoparticles are highly influenced by the preparation methods and conditions.

Keeping all these factors in view, we have demonstrated the ability of biosynthesized silver nanoparticles (Ag-NPs) from warm water extractions of *Tinospora Cordifolia* leaf extracts to use as flurorescence emitting probes.

II. Experimental

2.1 Biosynthesis of Ag-NPs.

Known weight (100 g) of *Tinospora Cordifolia* leaf powder (Figure. 1) was taken. Then it was placed in a 250 mL beaker containing 200 mL of distilled water. This was placed in boiling steam bath for 30 min until the color of the water changed to dark brown. The extract was cooled to room temperature, gently pressed and filtered through sterile serene cloth. This solution was treated as source extract and was utilized in subsequent procedures.

To the source extract, 40 mL of sterile organic-free water was added. The extract was treated with 20 mL of 0.025 M $AgNO_3$ solution and stirred until the color of solution changed and allowed to incubate in the laboratory ambience. The deposition gets distinctly visible in the flask which was left for 1-24 h and subsequently filtered. In present study, aqueous conditions were used in order to develop indeed green approach.

Figure 2 shows the UV-vis spectra of silver colloid obtained. The surface plasmon resonance (SPR) band is broad indicating poly-dispersed nanoparticles. A smooth and narrow absorption band at 440 nm is observed which is characteristic of mono-dispersed spherical nanoparticles. UV-visible spectroscopy is one of the most widely used techniques for structural characterization of silver nanoparticles. The surface plasmon resonance (SPR) band (λ max) around 440 nm broadened and slightly moved to the long wavelength region, indicating the presence and formation of silver nanoparticles. The optical absorption spectra of metal nanoparticles are

dominated by surface Plasmon resonances (SPR), which shift to longer wavelengths with increasing particle size.

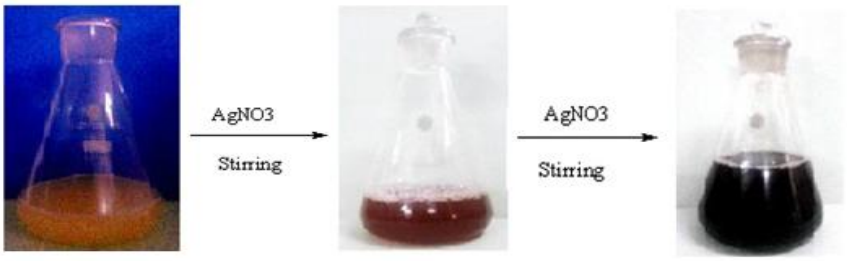

Figure 1. Synthesis of silver nano particals using aqueous *Tinospora cordifolia leaf* extract.

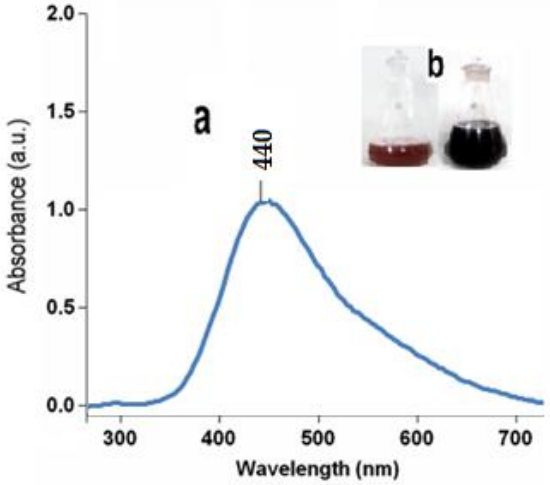

Figure 2: (a) UV-visual absorption spectra of silver nanoparticles after 24 h of reaction. (b) Picture of flask containing the solution of aqueous *Tinospora cordifolia leaf* extract filtrate with silver nitrate in Erlenmeyer flask, before reaction (flask 1) and after 24 h of reaction (flask 2).

2.2 Fluorescent studies

Fluorescence spectra were measured on a Schimadzu spectrofluorometer. The optical path was 1 cm and spectra were collected at a resolution of five data points per nanometer. The synthesized Ag-NPs (0.1 mmol) were dispersed in ammonia solution to study the photoluminescence activity using an excitation-emission matrix (EEM), which display fluorescence data. Excitation-emission matrices were created using MATLAB software. Fluorescence emission intensity is displayed over a range of excitation wavelengths.

III. Results and discussion:

3.1 Characterization

TEM micrograph of Ag-NPs was obtained on a F20 Tecnai High Resolution microscope (Philips, Netherlands). For TEM analysis, a few drops of the *Tinospora Cordifolia* leaf extract mediated silver solutions were placed onto a copper grid and dried overnight. The TEM images obtained silver colloid solution is shown in Figure 3. It can be seen that there are fairly dispersed and almost spherical shaped silver nanoparticles in Figure. 3a and b. Typical high resolution TEM images shows the oriented and ordered lattice fringes of silver nanoparticles. This confirms that the resulted silver nanoparticles are in a highly crystalline state.

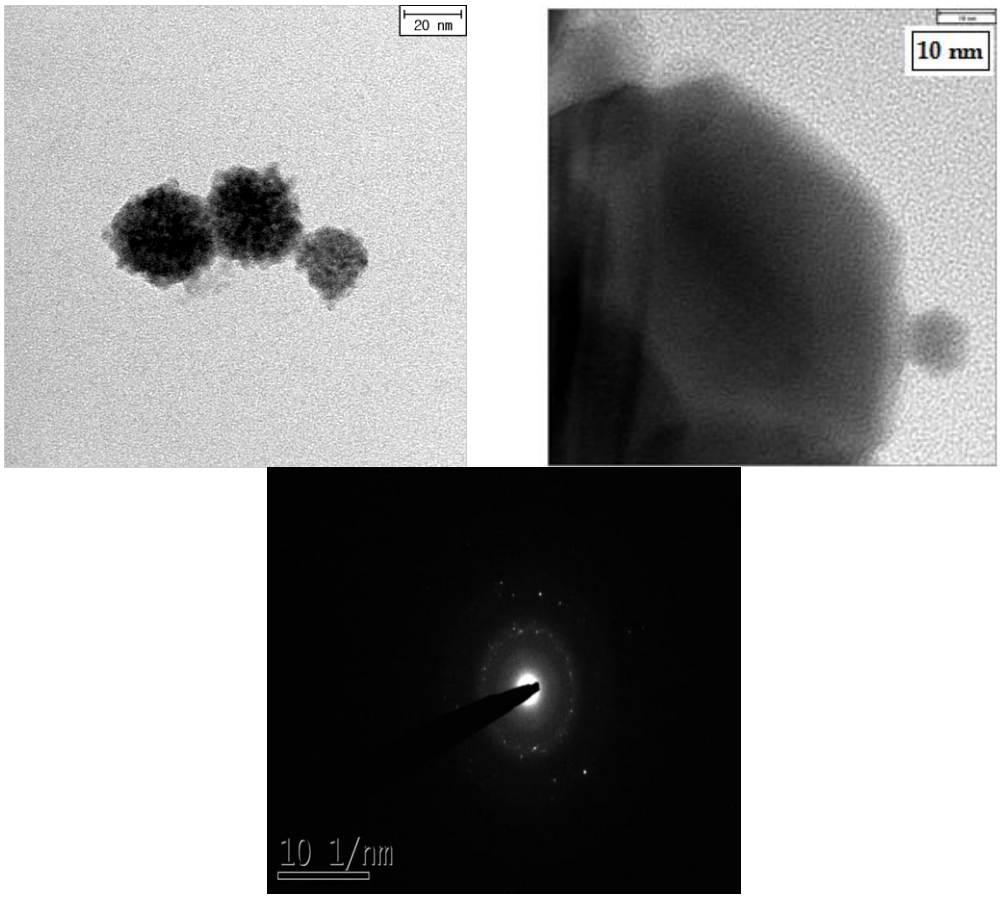

Figure 3: Transmission electron micrographs of the silver nanoparticles used in this work. (a) The bar marker represents 20 nm, (b) 10 nm & (C) HR-TEM micrograph at 2 nm showing spherical shape of silver nanoparticles .

X-ray diffraction (XRD) measurements were performed using a Rigaku D/MAX-RB conventional X–ray diffraction instrument operated at a voltage of 40 kV and a current of 100 mA with Cu Kα radiation. Figure 4 shows the XRD pattern of Ag-NPs obtained from *Tinospora Cordifolia* leaf extract. Diffraction peaks at two theta = 38.10, 44.65, 64.44 and 77.40^0 correspond to the indexed planes (111), (200), (220), and (311), respectively, which consistent to the fcc structure of the silver (JCPDS-CAS number 87-0720). In addition, the diffraction peaks in the XRD spectrum, two theta = 27.81, 28.90, 46.11, 54.42 and 58.81^0 suggesting that the oxide surface was formed on the surface of silver nanoparticles (JCPDS-CAS number 84-1261). The Scherrer analysis gave larger diffraction domains (about 21 nm), which is contradictory to TEM results. It is well-known that the interference factor was responsible in the classical XRD data interpretation of nanomaterials in poly-dispersion samples [24, 25]. The EDX spectrum (Figure 5) of Ag-NPs obtained from *Tinospora Cordifolia* leaf extract confirms the presence of silver.

FTIR measurements were carried out to identify the possible biomolecules responsible for stabilization of Ag-NPs synthesized using *Tinospora Cordifolia* leaf extract. FTIR spectra were recorded on the Shimadzu FTIR spectrometer with samples as KBr pellets. Figure 6 shows the FTIR spectrum of Ag-NPs obtained from *Tinospora Cordifolia* leaf extract. In FTIR spectrum, the absorption peaks at 3329, 1620, 1395, 1319 and 1049 cm^{-1}. The absorption peak 3329 cm^{-1} is attributed to the O—H stretching vibrations of alkaloids or steroids. The absorption peaks at 1620 and 1395 cm^{-1} indicates the C=O stretching vibration of fatty acids, and carboxylic O—H bending vibration of fatty acids, respectively. In the present study, the absorption peak corresponding to C=O stretching vibration of Tinosporin (~1700 cm^{-1}) is merged with 1620 cm^{-1} absorption peak. The absorption peaks observed at 1319 cm^{-1} and 1049 are due to C-O and C-O-C stretching vibrations, respectively. These findings suggest that the resulting silver nanoparticles might be stabilized by functional groups present in the biomolecules of *Tinospora Cordifolia* leaf extract such as Tinosporin and/or alkaloids. However, these findings are not sufficent to explain the exact mechanism of stabilization in this system. Further

investigations need to be carried out to propose the mechanism of present stabilization system.

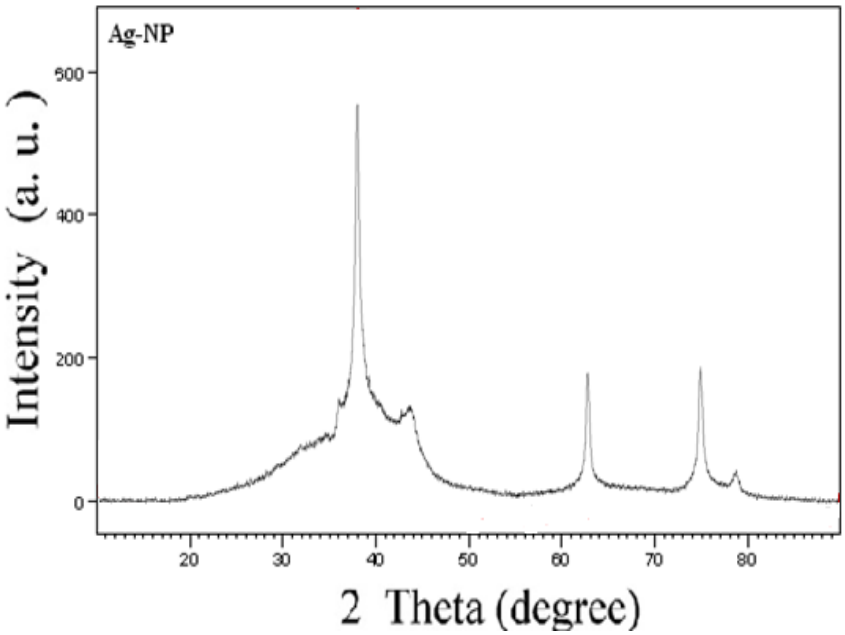

Figure 4. X-ray diffraction pattern of Ag-NP at room temperature synthesized by *Tinospora cordifolia* extract with $AgNO_3$ solution.

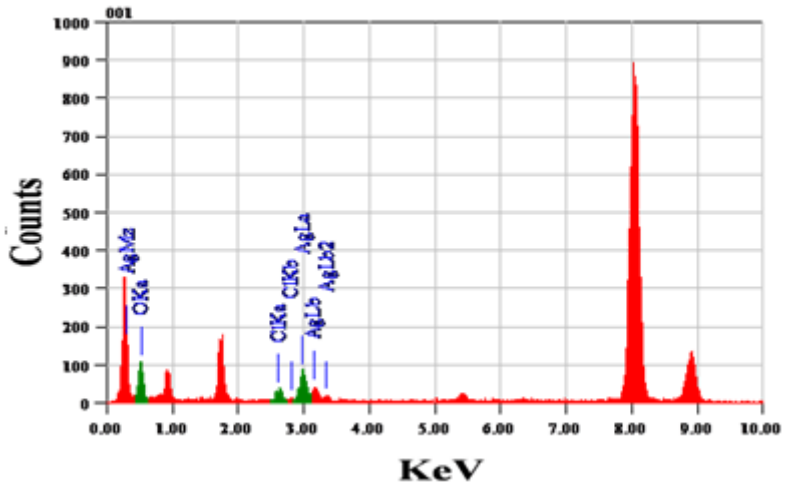

Figure 5. Energy-dispersive X-ray (EDX) spectrum of Ag-NPs from *Tinospora Cordifolia* leaf extract.

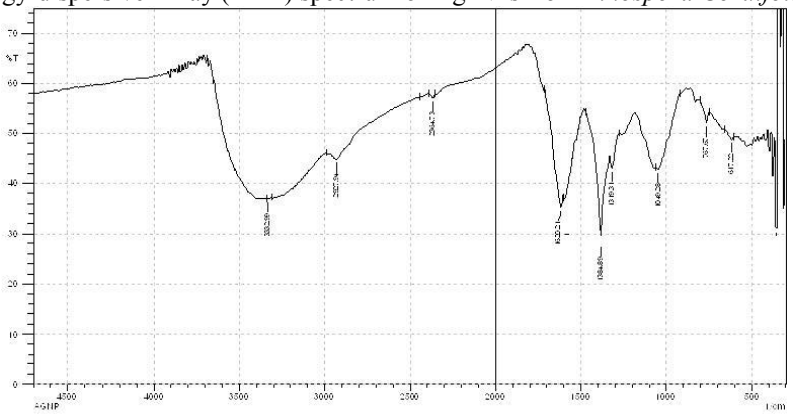

Figure 6. FT-IR spectra of *aqueous Tinospora cordifolia leaf extract* meaidted Ag-NPs.

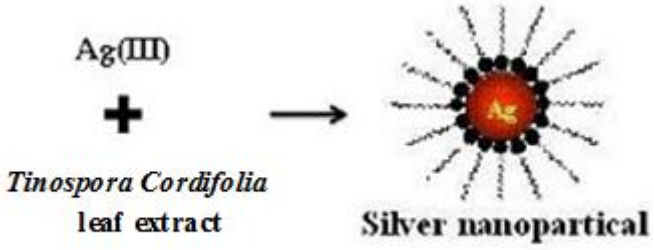

Scheme 1. Suggested mechanism showing the silver nanoparticles stabilized by the aqueous *Tinospora cordifolia leaf* extract.

3.4 Fluorescence studies.

Fluorescein has been used to derivatize biomolecules for decades, fluorescein-based dyes and their conjugates have several significant drawbacks, including: A relatively high rate of photobleaching, pH-sensitive fluorescence (pK_a ~ 6.4) that is significantly reduced below pH 7, A relatively broad fluorescence emission spectrum, limiting their utility in some multicolor applications, A tendency toward quenching of their fluorescence on conjugation to biopolymers, particularly at high degrees of labeling. Fluorescein's high photobleaching rate limits the sensitivity that can be obtained, a significant disadvantage for applications requiring ultrasensitive detection, such as DNA sequencing, fluorescence *in situ* hybridization and localization of low-abundance receptors. These limitations have encouraged us in the development of new alternative nano fluorophores.

Figure 9 shows the luminescence of Ag-NPs (0.01 % w/v) in ammonia solution at (a) daylight and (b) UV-lamp of 254 nm excitations respectively. Basing on this in view, fluorescence studies were carried on this Ag-NPs. Figure. 10 represent the emission spectra of Ag-NPs in ammonia solution. Detailed description with Stokes shifts were presented in table-1. Figures 11 display typical EEMs of Ag-NPs in ammonia. Peak locations and suggested fluorophores represented by them are provided in table 2. The scales of the EEMs listed are not consistent. The purpose of the following discussion is to identify *location* of fluorescent centers and compare those locations with previously identified peaks and their represented fluorophores.

The excitation range (300-500nm) and step interval (5nm) resulted in 41 excitation wavelength data points (300nm, 305nm, 310nm…. 500nm). Emission range (350-700nm) and step interval (5nm) resulted in 70 emission wavelength data points. Following the creation of EEMs, they were then exported into Excel files and later Sigma Plot files and MATLAB files for further interpretation and modeling. From the EEMs spectra location of the peak maxima was found to be: Ex. 340 nm/Em. 450 nm where fluorescence intensity is in Raman units.

Coagulation aggregates are easily formed due to Vander Waals forces or bonding between two clusters approaching each other. The presence of some amount of stabilizers such as Tinosporin in the explosion medium can terminate the aggregation. Ammonia as a medium will provide fast cooling for the generated particles with energetically favored shapes. Moreover, the high surface area per unit mass of the metal nanoparticle enhances the surface activity and tends to react with hydroxide molecules.

However, hydroxyl group of the ammonia have strong affinity to bind with electrons. This effect can be clearly observed by looking at the surface plasmon resonance (SPR) of the silver nanoparticles. The SPR signal as well as the fluorescence has been enhanced after the adsorption process. Electromagnetic excitation makes electrons at the higher occupied energy level (HOEL) undergo electronic transitions to the lower unoccupied energy level (LUEL) or excited states.

The interaction between the emissive centers and the interface environment has its signature on the observed fluorescence. One suggests that partial oxidations of metal nanoparticles lead to the formations of metal oxide clusters on the metal nanoparticle surface. These clusters at the surface are photo-activated by light excitations and might give rise to the observed fluorescence. Photo-activated fluorescence has been previously observed from small silver clusters [26].

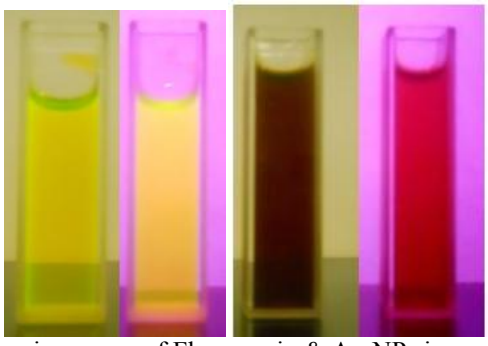

Figure. 9: The photos show the luminescence of Fluorescein & Ag-NPs in ammonia solution (a) daylight (Left) and (b) 254 nm excitations (Right), respectively.

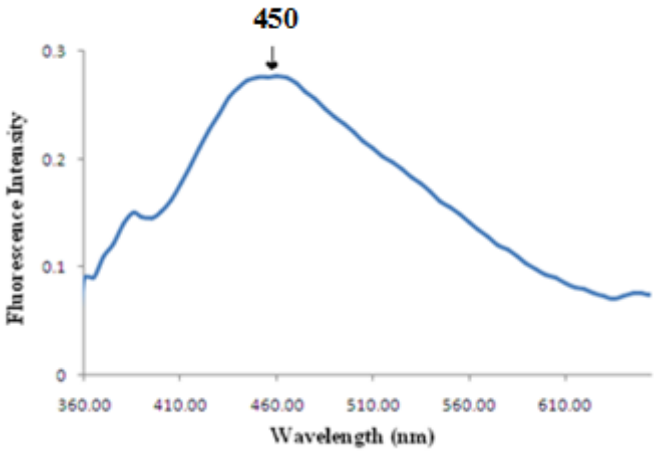

Figure. 10: Fluorescence emission of Ag-NPs in ammonia at 324nm excitation.

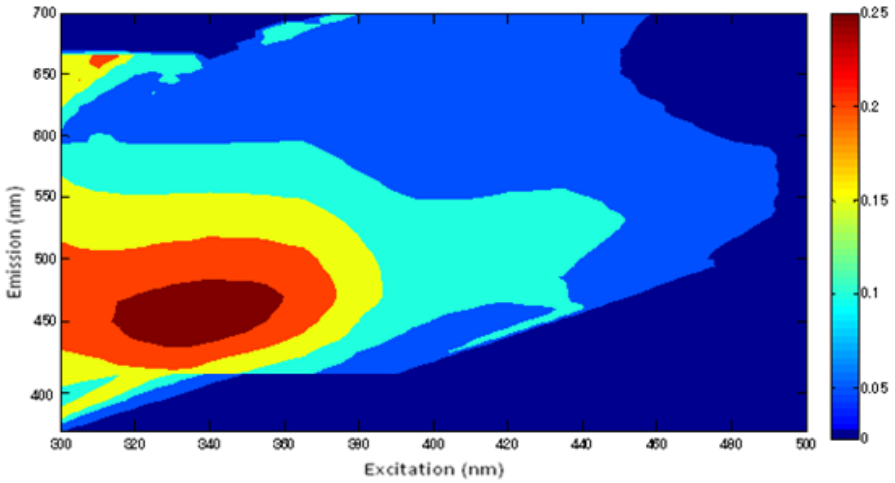

Figure. 11: Excitation–emission matrices for Ag-NPs in ammonia solution. Location of the peak maxima: Ex. 340 nm/Em. 450 nm. Fluorescence intensity in Raman units.

Table 1: Fluorescence Data of Ag-NPs in ammonia solution.

S. No	Fluorophore	Excitation wavelength (nm)	Emission wavelength (nm)	Stokes shift
01	Ag-NP	330	450	120

Table 2: Setup parameters for creation of EEMs

Parameter	
Scan Mode	Emission
Data Mode	Fluorescence
Excitation Wavelength Range (nm)	300 - 500
Excitation Step Invertval (nm)	5
Emission Wavelength Range (nm)	320 - 700
Emission Interval (nm)	5
Speed (nm/min)	12,000
Delay (s)	0
Excitation Shutter Opening (nm)	5
Emissiom Shutter Opening (nm)	5
PMT Voltage (V)	700
Response	Auto
Replicates	1
Shutter Control	ON
Spectrum Correction	ON

IV. Conclusions

This paper describes a green method for the synthesis of Ag-NPs. Further fluorescence studies were conducted to verify these particles as suitable bio markers. The results revealed describes these materials may act as fluorescent bio markers. In addition, Ag-NPs induced EEM fluorescence studies have been successfully exploited.

Acknowledgements

Authors are grateful to Andhra University, Visakhapatnam, India for support in Advanced Analytical Laboratories, A National facility, Andhra University for providing XRD & SEM.

References

[1.] Mukherjee, P. ; Ahmad, A.; Mandal, D.; Senapati, S.; Sainkar, S. R.; Khan, M. I.; Parishcha, R.; Ajaykumar, P. V.; Alam, M.; Kumar, R.; Sastry, M . Fungus-Mediated Synthesis of Silver Nanoparticles and Their Immobilization in the Mycelial Matrix: A Novel Biological Approach to Nanoparticle Synthesis. *Nano Lett.* **2001**, *1*, 515–519.

[2.] Ahmad, A.; Mukherjee, P.; Mandal, D.; Senapati, S.; Khan, M. I.; Kumar, R.; Sastry, M.. Enzyme Mediated Extracellular Synthesis of CdS Nanoparticles by the Fungus, *Fusarium oxysporum. J. Am. Chem. Soc.* **2002**, *124*, 12108–12109.

[3.] Sastry, M.; Ahmad, A.; Khan, M. I.; Kumar, R . Bio synthesis of metal nanoparticles using fungi and actinomycete. *Curr. Sci*. **2003**, *85*, 162–170.

[4.] Shankar, S. S.; Ahmad, A.; Sastry, M . Geranium leaf assisted biosynthesis of silver nano particles. *Biotechnol. Prog.* **2003**, *19*, 1627–1631.

[5.] Shankar, S. S.; Rai, A.; Ankamwar, B.; Singh, A.; Ahmad, A.; Sastry, M . Biological synthesis of triangular gold nanoprisms. *Nat. Mater.* **2004**, *3*, 482– 488.

[6.] Rai, A.; Singh, A.; Ahmad, A.; Sastry, M . Role of Halide Ions and Temperature on the Morphology of Biologically Synthesized Gold Nano triangles. *Langmuir*. **2006**, *22*, 736–741.

[7.] Vineet, K.; Sudesh, K.Y. Plant-mediated synthesis of silver and gold nanoparticles and their applications. *J. Chem. Technol. Biotechnol.* **2009**, *84*, 151-157.

[8.] Majid, D.; Mansor, B. Ahmad,; Reza Zamiri,; AK Zak,; Abdul. H. Abdullah,; Nor Azowa Ibrahim. Time-dependent effect in green synthesis of silver nano particles. *International Journal of Nanomedicine.* **2011**, *6*, 677-681.

[9.] Tamizhamudu, E.; Kantha D Arunachalam. *Memecylon edule* leaf extract mediated green synthesis of silver and gold nanoparticles. *Inter. Journal of Nanomedicine*. **2011**, *6*, 1265-1278.

[10.] Majid Darroudi.; Ali. K. Zak.; Muhamad, M. R.; Huang, N. M.; Mohammad Hakimi. Green synthesis of colloidal silver nanoparticles by sonochemical method. *Materials Letters*. **2012**, *66*, 117-120.

[11.] Tolaymat, T. M.; Amro. M. El Badawy.; Genaidy, A.; Scheckel, K. G.; Luxton, T. P.; Makram Suidan. An evidence-based

environmental perspective of manufactured silver nano particle in syntheses and applications: A systematic review and critical appraisal of peer-reviewed scientific papers. *Science of the Total Environment.* **2010**, *408*, 999-1234.

[12.] Aruna Jyothi, K.; Arunachalam. J. Leaf Extract of *Dendrophthoe falcata*: A Renewable Source for the Green Synthesis of Antibacterial Silver Nanoparticles. *Journal of biobased Materials and Bioenergy.* **2012**, *6(2)*, 158-164.

[13.] Konwarh, R.; Gogoi, B.; Philip, R.; Laskar, M.A.; Niranjan, K. Biomimetic preparation of polymer-supported free radical scavenging, cytocompatible and antimicrobial "green" silver nanoparticles using aqueous extract of Citrus sinensis peel. Colloids and Surfaces B: Biointerfaces. **2011**, *84(2)*, 338-345.

[14.] Kamat, P. V . Photophysical, Photochemical and Photocatalytic Aspects of Metal Nanoparticles. *J Phys Chem B.* **2002**, *106(32)*, 7729-7744.

[15.] Lakowicz, J. R . Radiative Decay Engineering: Biophysical and Biomedical Applications. *Anal Biochem*. **2001**, *298*, 1-24.

[16.] Lakowicz, J. R.; Shen, Y.; D'Auria, S.; Malicka, J.; Fang, J.; Gryczynski, Z.; Gryczynski, I . Radiative Decay Engineering: 2. Effects of Silver Island Films on Fluorescence Intensity, Lifetimes, and Resonance Energy Transfer. *Anal Biochem*. **2002**, *301*, 261-277.

[17.] Lakowicz, J. R . Radiative decay engineering 3. Surface plasmon-coupled directional emission. *Anal Biochem.* **2004**, *324*, 153-169.

[18.] Aslan, K.; Cryczynski, I.; Malicka, J.; Lakowicz, J. R.; Geddes, C. D . Metal-enhanced fluorescence: an emerging tool in biotechnology. *Curr Opin Biotechnol.* **2005**, *16(1)*, 55-62.

[19.] Aslan, K.; Holley, P.; Davies, L.; Lakowicz, J. R.; Geddes, C. D . Angular-ratiometric plasmon-resonance based light scattering for bioaffinity sensing. *J Am Chem Soc.* **2005**, *127*, 12115-12121.

[20.] Zhang, J.; Matveeva, E.; Gryczynski, I.; Leonenko, Z.; Lakowicz, J. R . Metal-Enhanced Fluoroimmunoassay on a Silver Film by Vapor Deposition. *J Phys Chem B.* **2005**, *109*, 7969-7975.

[21.] Zhang, J.; Malicka, J.; Gryczynski, I.; Lakowicz, J. R . Surface-Enhanced Fluorescence of Fluorescein-Labeled Oligonucleotides Capped on Silver Nanoparticles. *J Phys Chem B.* **2005**, *109*, 7643-7648.

[22.] Corrigan, T. D.; Guo, S.; Phaneuf, R. J.; Szmacinski, H . Enhanced fluorescence from periodic arrays of silver nanoparticles. *J Fluoresc.* **2005**, *15*, 777-784.

[23.] Haes, A. J.; Stuart, D. A.; Nie, S.; Van Duyne, R. P . Using solution-phase nanoparticles, surface-confined nanoparticle arrays and single nanoparticles as biological sensing platforms. *J Fluoresc.* **2004**, *14*, 355-367.

[24.] Langford, J. I.; Louer, D.; Scardi, P . Effect of a crystallite size distribution on X-ray diffraction line profiles and whole-powder-pattern fitting. *J. Appl. Crystallogr*. **2000**, *33*, 964-974.

[25.] Amato, E.; Diaz-Fernandez, Y. A.; Taglietti, A.; Pallavicini, P.; Pasotti, L.; Cucca, L.; Milanese, C.; Grisoli, P.; Dacarro, C.; F-Hechavarria, J. M.; Necchi, V . Synthesis, Characterization and Antibacterial Activity against Gram Positive and Gram Negative Bacteria of Biomimetically Coated Silver Nanoparticles. *Langmuir*. **2011**, *27*, 9165-9173.

[26.] Peyser, L. A.; Vinson, A. E.; Bartko, A. P.; Dickson, R. M . Photoactivated Fluorescence from Individual Silver Nanoclusters. *Science*. **2001**, *291*, 103-106.